Contribution from the Departments of Chemistry, McMaster University, Hamilton, Ontario L8S 4M1, Canada, and The University of Leicester, Leicester LE1 7RH, England

Preparation and Study by Raman Spectroscopy of $KrF_2 \cdot MOF_4$, $XeF_2 \cdot MOF_4$, and $XeF_2 \cdot 2MOF_4$ (M = Mo, W) and a Solution ^{19}F NMR Study of $KrF_2 \cdot nMoOF_4$ (n = 1-3) and $KrF_2 \cdot WOF_4$

JOHN H. HOLLOWAY[1a] and GARY J. SCHROBILGEN*[1b]

Received December 3, 1980

The first krypton difluoride–metal oxide fluoride adducts have been prepared by reaction of KrF_2 with MOF_4 (M = Mo, W) in SO_2ClF solution at low temperatures. The ^{19}F NMR spectra of $KrF_2 \cdot nMoOF_4$ (n = 1–3) and $KrF_2 \cdot WOF_4$ in solution show that they are best formulated as essentially covalent structures containing Kr---F---M bridges and mononuclear or polynuclear metal oxide fluoride moieties. Studies of equilibria involving Kr–O–W- and Kr---F---W-bridged species have been interpreted to suggest that stable krypton–oxygen bonds are unlikely. Raman spectra of the solid $KrF_2 \cdot MOF_4$ (M = Mo, W) adducts have been compared with those of the analogous xenon compounds and all have been interpreted in terms of covalent fluorine-bridged structures. The Raman spectra of the solid adducts $XeF_2 \cdot 2MOF_4$ are also reported.

Introduction

Our recent studies of the fluoride ion acceptor properties of WOF_4 and $MoOF_4$ toward XeF_2 have shown that stable adducts with stoichiometries $XeF_2 \cdot MOF_4$ and $XeF_2 \cdot 2MOF_4$ (M = Mo, W) exist.[2] Their ^{19}F and ^{129}Xe NMR spectra in BrF_5 and SO_2ClF solvents have shown that the adducts contain Xe---F---M bridges which are nonlabile on the NMR time scale at low temperatures and, as such, have provided the first evidence of such bridges in solution. Equilibria involving higher chain-length species such as $XeF_2 \cdot nMOF_4$ (n = 3, 4), in addition to the $XeF_2 \cdot MOF_4$ and $XeF_2 \cdot 2MOF_4$ entities, have also been observed at low temperatures in SO_2ClF solution.

In the present paper, KrF_2 analogues have been synthesized and their solution structures in SO_2ClF solvent have been studied at low temperatures. In view of the fact that the XeF_2 adducts of WOF_4 undergo

bond isomerization at low temperatures in SO_2ClF media, the possibility of a similar isomerization reaction occurring for KrF_2 adducts of WOF_4 has been investigated. This was considered important since it might provide the first evidence of a Kr–O bond.

Results and Discussion

^{19}F NMR Spectroscopy. $KrF_2 \cdot nMoOF_4$. Solutions of KrF_2 and $MoOF_4$ of different relative compositions in SO_2ClF solvent have been found to be stable below 0 °C and contain equilibrium mixtures of $KrF_2 \cdot nMoOF_4$ (n = 1–3) at -121 °C. As in the case of the XeF_2 analogues,[2] ^{19}F NMR spectra show that the KrF_2 molecule is fluorine bridged to the molybdenum (structures I–III). Thus, two fluorine-on-krypton environments are observed for each structure. These environments are distinguished by their accompanying spin–spin coupling patterns. A doublet, F_a, and a higher field doublet of quintets, F_b, are observed for each structure (Figures 1a,b and 2). The doublet is readily assigned to the lower field terminal fluorine on krypton, F_a, spin–spin coupled to F_b. By altering the initial relative amounts of KrF_2 and $MoOF_4$ and observing the effects on relative intensities of the fluorine-on-krypton environments in the ^{19}F NMR spectra at equilibrium at low temperature (Table I), it has been possible to assign the terminal fluorine-on-krypton resonances to their respective mononuclear and polynuclear molybdenum species (Figures 1a and 2 and structures I–III).

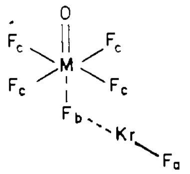

I

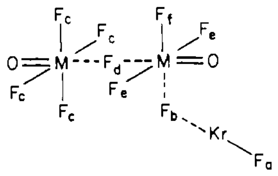

II

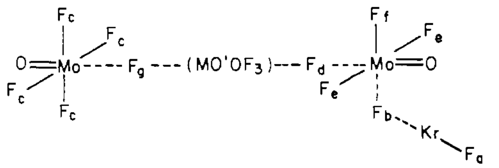

III

Table I. ^{19}F NMR Parameters for $KrF_2 \cdot nMoOF_4$ (n = 1-3) and $KrF_2 \cdot WOF_4$ in SO_2ClF Solution at -121 °C

species (structure)[a]	$\delta\,{}^{19}F$[b]	J_{F-F}, Hz
FKrF--$MoOF_4$ (I)	F_a 70.4 F_b -12.4 F_c 148.6	F_a-F_b 296 F_b-F_c 44
FKrF--$MoOF_4(MoOF_4)$ (II)	F_a 64.9 F_b -28.8 F_c 150.1 F_d -34.8 F_e 190.8 F_f 208.5	F_a-F_b 314 F_b-F_d 48 F_b-F_e 52 F_b-F_f 44 F_c-F_d 44 F_d-F_e 92 F_d-F_f 110 F_e-F_f 100
FKrF--$MoOF_4(MoOF_4)_2$ (III)	F_a 65.4 F_b -31.1 F_c 150.5 F_d 14.6 F_e 0 F_f 0 F_g 10.8 F on M' [c]	F_a-F_b 326 F_b-F_c ~50
FKrF--WOF_4 (I)	F_a 67.7 F_b -26.1 F_c 67.9	F_a-F_b 311 F_b-F_c 48

[a] Observed mole ratios of $KrF_2 \cdot nMoOF_4$: KrF_2:$MoOF_4$ = 1.00, I:II:III = 1.00:0.11:0.02; KrF_2:$MoOF_4$ = 0.67, I:II:III = 1.00:0.15:0.11; KrF_2:$MoOF_4$ = 0.40, I:II:III = 1.00:0.80:0.55. [b] ^{19}F Chemical shifts are with respect to $CFCl_3$ at the sample temperature. Positive values denote chemical shifts to low field of the reference and vice versa. [c] These resonances overlap severely with F_e and F_f of structure II.

The 1:1 adducts can be satisfactorily represented by the valence bond structures IVa–IVc. Analogous structures can be written for species containing polynuclear MOF_4 moieties. The assignments and chemical shift trends are consistent with the anticipated relative order of basicities of the corresponding mono- and polynuclear anions, giving rise to greater KrF^+ character (decreasing frequency), as represented by structure

---

[1] (a) University of Leicester. (b) McMaster University; presented the portion of this work on krypton chemistry at the IXth International Symposium on Fluorine Chemistry, Avignon, France, 1979.

[2] Holloway, J. H; Schrobilgen, G. J. *Inorg. Chem.* **1980**, *19*, 2632.

0020-1669/81/1320-3363$01.25/0

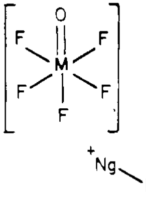

IVa

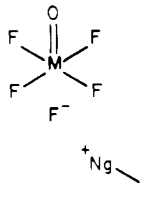

IVb

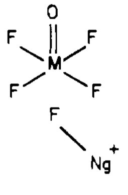

IVc

IVa, for the terminal KrF group with decreasing basicity (increasing chain length) of the poly(oxotetrafluoromolybdenum) group (Figure 2). The shielding trend is also consistent with enhancement of the KrF^+ (two-center–two-electron bond) character of the terminal Kr–F bond relative to that of KrF_2 (three-center–four-electron bonds, i.e., only one bonding pair of electrons is available for two Kr–F bonds). In general, the effects of decreasing basicity of the polynuclear chains are noted to attenuate rapidly with increasing chain length. The observed trends and assignments are supported by the previous observation that increased shielding occurs upon ionization of KrF_2 (55.6 ppm) in HF to give KrF^+ (−22.6 ppm).[3]

The corresponding series of bridging environments, F_b, occur at lower frequencies and display spin–spin coupling to the terminal fluorine-on-krypton and adjacent fluorine-on-molybdenum environments. The fine structure on the bridging fluorines consists of a doublet of 1:4:6:4:1 quintets for structure I and a doublet of pseudoquintets for structures II and III. This indicates that coupling between the bridging fluorine on krypton and the fluorines on the adjacent molybdenum are nearly all equal in structures II and III (Figure 1b and Table I). For the latter structures, partial overlap occurs between these bridging environments. It is also notable that the chemical shift of the bridging fluorine on krypton is more sensitive to the length of the poly(oxotetrafluoromolybdenum) chain than the corresponding environment in its xenon analogue.[2]

The fluorine–fluorine spin–spin couplings, F_a–F_b, are similar in magnitude to those reported for $Kr_2F_3^+$ (329 Hz),[3] the (μ-F)$XeF_2 \cdot nMOF_4$ (M = Mo, W; n = 1–4) analogues (258–275 Hz),[2] and $Xe_2F_3^+$ (308 Hz).[4] It has been noted previously, that, with the exception of $Xe_2F_3^+$, fluoro and oxyfluorocations of xenon possess comparatively small fluorine–fluorine coupling constants (103–176 Hz).[5] The large difference is likely to be associated with the size of the F–Ng---F (Ng = Kr or Xe) angle which is near linear in $Ng_2F_3^+$ and (μ-F)$NgF_2 \cdot nMOF_4$ but ~90° in the other cations. It is also noteworthy that the bridging resonances of the (μ-F)$KrF_2 \cdot nMoOF_4$ species, like that of $Kr_2F_3^+$, occur to high field of their respective terminal fluorine on krypton resonances. This trend is opposite to that displayed by $Xe_2F_3^+$, (μ-F)$XeF_2 \cdot nWOF_4$ and (μ-F)$XeF_2 \cdot nMoOF_4$.[2]

The existence of polymeric chains comprising of up to three $MoOF_4$ molecules, linked together by Mo---F---Mo bridges, is further confirmed by the observation of the fluorine on molybdenum resonances. The fluorine on molybdenum environments, F_c, which occur at significantly higher frequencies than fluorine on krypton environments, appear as simple first-order doublets in the ^{19}F NMR spectra (Figure 1c). The doublet fine structures associated with F_c of structures II and III confirm that all of the adduct chains terminate in a $MoOF_4$ group with the oxygen trans to the adjacent Mo---F---Mo fluorine bridge. The ^{19}F resonance of the terminal $MoOF_4$ groups of structures II and III are all near-coincident as evidenced by increased skewing and concomitant loss of resolution on the low-field doublet with increasing relative proportions of $MoOF_4$. Analogous chemical shift behavior was observed for the XeF_2 compounds where chemical shifts of terminal $MoOF_4$ groups ranged from 147.7 to 150 ppm.[2]

The Mo---F---Mo bridge environments are less shielded than their counterparts in $Mo_2O_2F_9^-$ (−135 ppm in propylene carbonate solution). The Mo---F---Mo bridging fluorine environment of the 1:2 structure is well separated and is similar to that found in the XeF_2 analogue (−37.7 ppm).[2] Fine structure resolved on F_d in structure II consists of a ten-line nonbinomial multiplet (Figure 1b) whose coupling constants have been estimated (Table I) by assuming the geometry represented by structure II. The remaining fluorine on molybdenum environments, F_e and F_f of structure II, have been assigned to two low-field multiplets with rather similar chemical shifts. These multiplets have been assigned on the basis of their relative intensities (Figure 1d and Table I) and are in good agreement with the corresponding assignments in the XeF_2 analogue (F_e, 195.1 ppm and F_f, 207.9 ppm). The spin–spin coupling patterns for this portion of the spectrum have been fitted with use of the NMR simulation program NUMARIT[6] and are reported in Table I.

The low-field fluorine-on-molybdenum environments of structures II and III, i.e., F_c, F_e, F_f, and fluorines on Mo, severely overlap with one another; consequently, no chemical shifts or coupling constants are reported. The bridging fluorines F_d and F_g of structure III are, however, well separated but are broad and lacking in fine structure.

$KrF_2 \cdot nWOF_4$. Solutions of KrF_2 and WOF_4 in SO_2ClF are highly unstable above −100 °C, and Kr and O_2 gases are rapidly evolved according to eq 1. The ^{19}F resonance arising

$$KrF_2 + WOF_4 \rightarrow Kr + {}^{1}/_{2}O_2 + WF_6 \qquad (1)$$

from WF_6 was detected at 164.7 ppm in SO_2ClF (−121 °C). In addition, a set of resonances attributable to (μ-F)$KrF_2 \cdot WOF_4$ was also observed (Table I). The spectrum is readily assigned by comparison with the (μ-F)$KrF_2 \cdot MoOF_4$ analogue discussed above. There was no evidence for $KrF_2 \cdot nWOF_4$ (n > 1) even in the presence of initially large excesses of WOF_4.

The (μ-F)$KrF_2 \cdot nMoOF_4$ (n = 1–3) adducts are stable up to room temperature in SO_2ClF solution (see section on Raman spectroscopy). The tendency of WOF_4 to undergo oxidative fluorination with KrF_2 in SO_2ClF solvent at room temperature, therefore, is in complete contrast to the $MoOF_4$ case. It appears that the nature of adduct formation plays an important role in this difference in behavior. In the XeF_2/WOF_4 adduct system in SO_2ClF

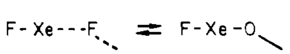

bond isomerizations have been shown to occur for $XeF_2 \cdot nWOF_4$, where n > 1, but do not occur with either $MoOF_4$ analogues or $XeF_2 \cdot WOF_4$.[2] The equilibrium constant of eq 2, where K_n has been measured for n = 1–3, is 0 when n = 1 and increases by roughly a factor of 10 for each subsequent increment of n at −121 °C. We suggest, therefore, that the marked difference in oxidizability of $MoOF_4$ and WOF_4 by KrF_2 in these solutions may well be due to an analogous

$$K_n = \frac{[(\mu\text{-O})XeF_2 \cdot nWOF_4]}{[(\mu\text{-F})XeF_2 \cdot nWOF_4]} \qquad (2)$$

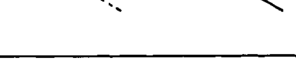

---

(3) Gillespie, R. J.; Schrobilgen, G. J. *Inorg. Chem.* **1976**, *15*, 22.

(4) Gillespie, R. J.; Netzer, A.; Schrobilgen, G. J. *Inorg. Chem.* **1974**, *13*, 1455.

(5) Gillespie, R. J.; Schrobilgen, G. J. *Inorg. Chem.* **1974**, *13*, 2370.

(6) Haigh, C. W.; Harris, R. K.; Martin, J. S. "NMR Spectral Analysis Program NUMARIT", private communication.

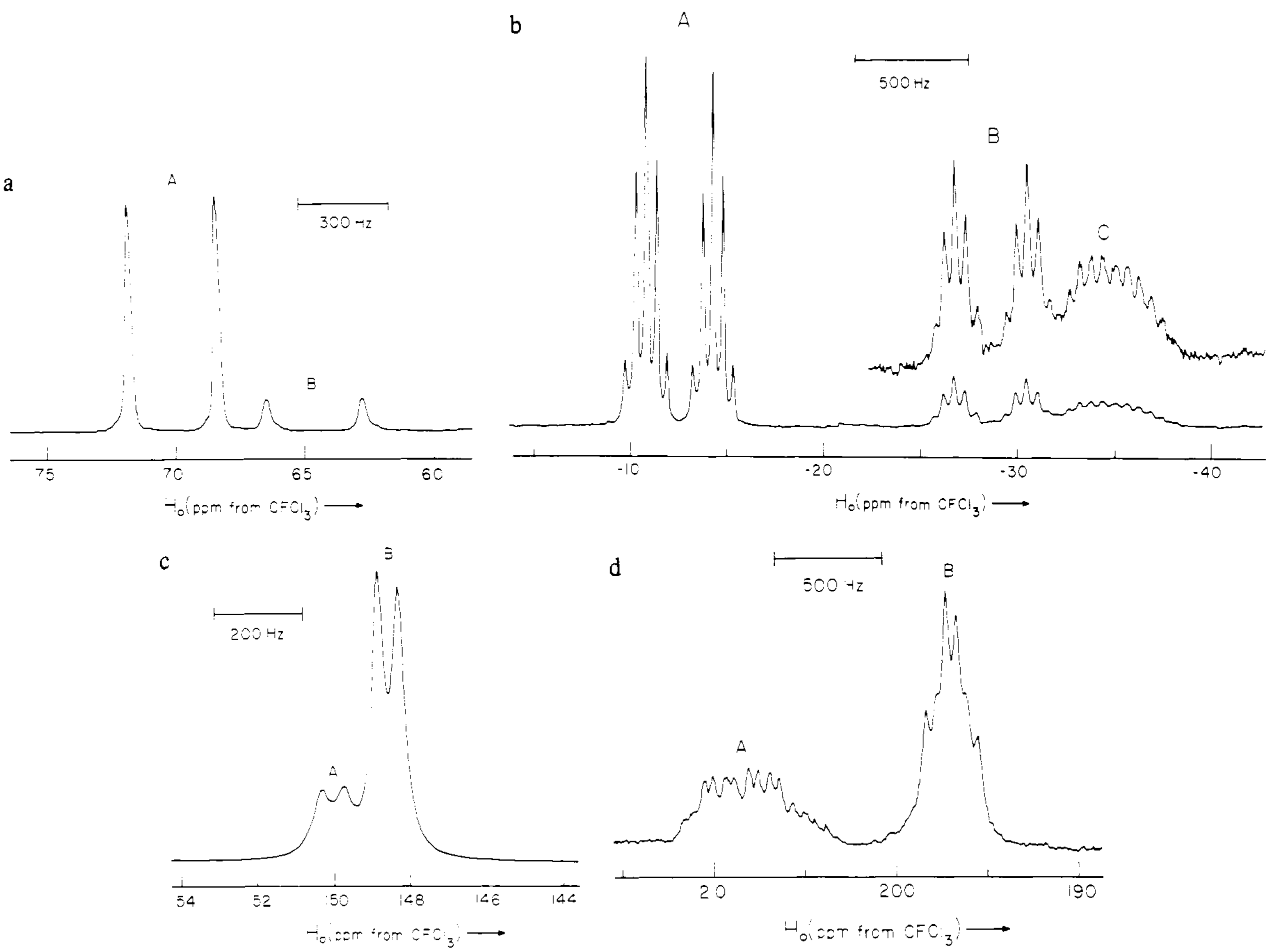

Figure 1. Pulse FT ^{19}F NMR spectra (−127 °C, 84.66 MHz) for an equilibrated mixture of KrF_2 (0.20 *m*) and $MoOF_4$ (0.25 *m*), $MoOF_4/KrF_2 = 1.2$ in SO_2ClF solvent: (a) terminal fluorine on krypton environments of A, structure I, and B, structure II; (b) bridging fluorine on krypton environments of A, structure I, and B, structure II (multiplet C is assigned to F_d of structure II); (c) terminal $MoOF_4$ environments, F_c, for A, structure I, and B, structure II; (d) nonterminal fluorine on molybdenum environments of structure II where multiplet A is assigned to F_f and multiplet B is assigned to F_e.

bond isomerization process in $KrF_2 \cdot nWOF_4$ ($n > 1$) represented in reaction 3. Analogous isomerizations in the

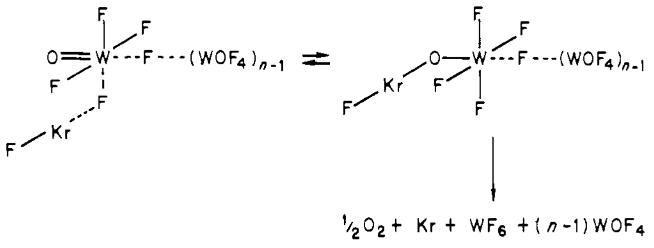

(3)

KrF_2/WOF_4 system would account for the stability of (μ-F)$KrF_2 \cdot WOF_4$ and its subsequent isolation from SO_2ClF solution (see section on Raman spectroscopy) as well as the instability of $KrF_2 \cdot nWOF_4$ ($n > 1$). Equilibrium amounts of Kr–O-bonded polynuclear tungsten species are apparently thermally unstable under the conditions cited and decompose according to the redox reaction given in eq 3.

The detection of only $F_5TeOOTeF_5$ in the reactions of KrF_2 with $B(OTeF_5)_3$ at low temperature has been cited as evidence that the synthesis of a stable compound containing a Kr–O bond is unlikely.[7] Our present results give further credence to these suggestions.

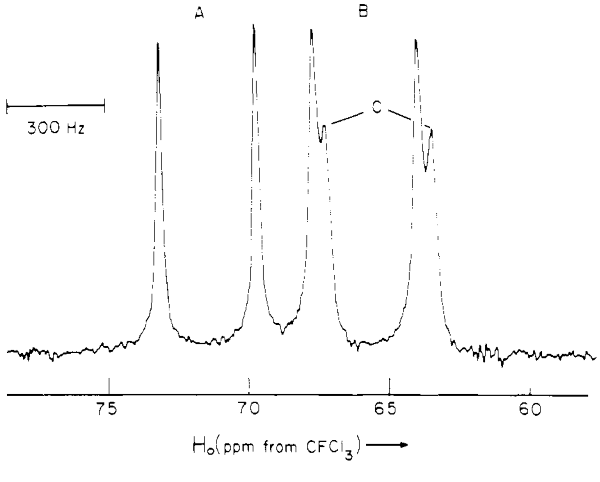

Figure 2. Pulse FT ^{19}F NMR spectrum (−127 °C, 84.66 MHz) for an equilibrated mixture of KrF_2 (0.43 *m*) and $MoOF_4$ (1.06 *m*), $MoOF_4/KrF_2 = 2.47$ in SO_2ClF solvent (only the terminal fluorine on krypton regions are depicted): A, structure I; B, structure II; C, structure III.

Raman Spectroscopy

$KrF_2 \cdot MoOF_4$, $KrF_2 \cdot WOF_4$, $XeF_2 \cdot MoOF_4$, and $XeF_2 \cdot WOF_4$. The Raman spectra of the title compounds are given in Figures 3 and 4 and Table II. The X-ray crystal structure of $XeF_2 \cdot WOF_4$ shows that the adduct possesses C_s symmetry with a rather long contact distance between the tungsten atom and

---

[7] (a) Keller, N.; Schrobilgen, G. J., unpublished observations. (b) Lentz, D.; Seppelt, K. *Angew. Chem., Int. Ed. Engl.* **1979**, *18*, 66.

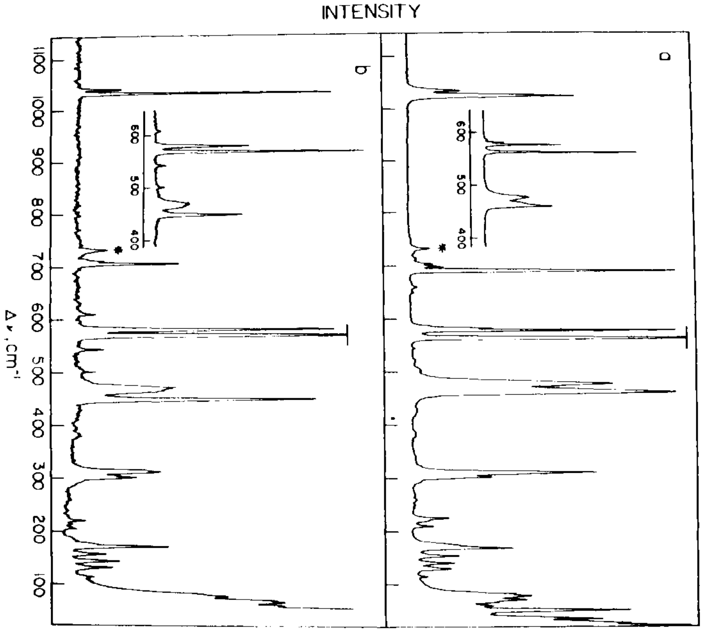

Figure 3. Raman spectra (−196 °C) of (a) $KrF_2·MoOF_4$ and (b) $KrF_2·WOF_4$ (asterisk denotes an FEP sample tube line).

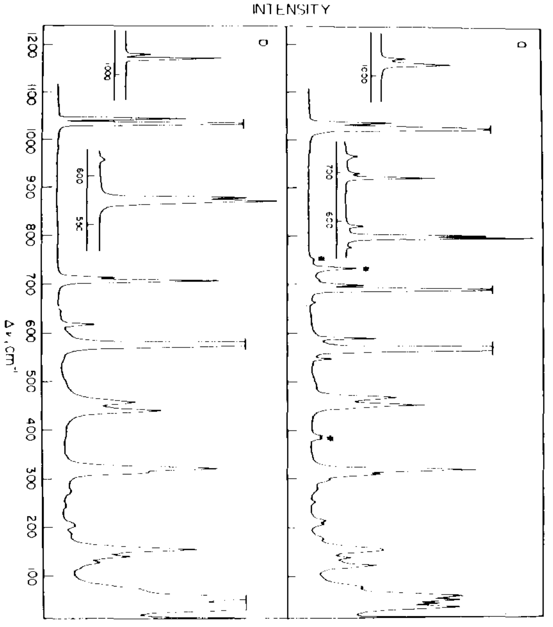

Figure 4. Raman spectra of (a) $XeF_2·MoOF_4$ (−100 °C) and (b) $XeF_2·WOF_4$ (−80 °C) (asterisks denote FEP sample tube lines).

the nearest-neighbor fluorine bonded to xenon (2.18 Å in structure I).[8] In view of the 1:1 correspondence of the lines in the Raman spectra of $KrF_2·MOF_4$ and $XeF_2·MOF_4$ (M = Mo, W), attempts had initially been made to assign the spectra of all these adducts on the basis of C_s symmetry. The adduct $XeF_2·WOF_4$ belongs to the crystallographic space group $P2_1/c$ with $Z = 4$. A factor-group analysis using this space group reveals that a maximum of two lines per mode (an a_g and a b_g component) are expected due to vibrational coupling within the unit cell. A total of 21 Raman-active bands corresponding to the irreducible representation 14 a′ + 7 a″ are expected. Excluding the expected factor-group splittings on each line, considerably less than this number of lines was actually observed (Table II). The spectral assignments have therefore

Table II. Vibrational Frequencies (cm^{-1}) and Assignments for $KrF_2·MOF_4$ and $XeF_2·MOF_4$ Compared to Those of the MOF_5^- Anion (M = Mo, W)

NO^+MoOF_5 [a]		$Cs^+MoOF_5^-$ [b]		FKrF--$MoOF_4$ [c]	FXeF--$MoOF_4$ [d]	$NO^+WOF_5^-$ [a]		$Cs^+WOF_5^-$ [b]		FKrF--WOF_4 [c]	FXeF--WOF_4 [d]	
IR	R	IR	R	R	R	IR	R	IR	R	R	R	assignt and approx descriptn
990 s	985 (100)	973 vs	973 vs	1034 (12), 1025 (33)	1036 (12), 1024 (35)	1003 s	1001 (100)	987 vs	989 vs	1041 (8), 1034 (45)	1043 (14), 1033 (56)	a_1, ν(M=O)
	665 (72)	662 vw	666 m	698 (7), 691 (63)	698 (8), 689 (47)	680 sh	684 (35)	686 s	689 s	712 (4), 706 (18)	714 (6), 706 (8)	a_1, ν(sym in-plane MF_4)
650 vs		605 vs		702 (5), 661 (2)	716 (1), 662 (0.5)	610 vs		608 vs		611 (3)	618 (4)	e, ν(asym in-plane MF_4)
550 sh	557 (6)		(580)	582 (16)	588 (9)		591 (4)		594 vw	544 (5)		b_1, ν(sym out-of-phase MF_4)
					546 (3)							
					509 (0.5)					504 (4)		
436 ms		492 m		462 (59)	466 (12)	455 m		507 m		450 (42)	458 (8)	a_1, ν(axial MF)
317 (62)			324 m	312 (36)	316 (24)		327 (59)	329 s	331 m	312 (16)	320 (17)	e, δ(MOF_4)
				260 (1)	277 (1), 251 (1)						274 (1), 248 (0.5), 241 (0.5)	b_2, δ(MF_4)
293 (1)		300 w		303 (15)	307 (10)		292 sh	286 m	287 vs	301 (12)	311 (sh)	a_1, δ(MF_4)
		252 s		226 (7), 220 sh, 210 (4)	212 (2), 204 (2)			242 s		221 (4), 206 (2)	206 (1), 202 (1)	e, δ(MF_4)
				174 sh	174 (3)							b_1, δ(MF_4)
				155 (8), 140 (8)	152 (10),[f] 136 (5)					158 (6), 144 (8)	153 (14),[f] 139 (6)	e, δ(FMF_4)
				579 (53), 566 (100)	575 (75), 566 (100)					571 (100), 581 (45)	573 (100), 577 (83)	Σ^+, ν(Ng–F)
				479 (40)	451 (16)					469 (17)	439 (11)	Σ^+, ν(Ng--F)
				170 (20)	152 (10)[f]					172 (18)	153 (14)[f]	π, δ(F–Ng--F)
				130 (6), 116 (2), 84 sh, 79 (17), 72 (15), 69 sh, 60 (5), 52 (30), 37 (12), 29 (6)	119 (9), 74 (5), 55 (18), 46 (17), 39 (14), 31 (16)					132 (7), 115 (3), 78 (10), 68 (12)	127 (3), 70 (5), 53 (18), 35 (25), 30 sh	lattice modes

[a] Reference 12. [b] Reference 11. [c] Recorded at −196 °C in an FEP sample tube. [d] Recorded at −108 °C in an FEP sample tube. [e] The MOF_5^- anion and MOF_5 moiety of the adducts are assigned on the basis of assumed C_{4v} symmetry. The linear F–Ng—F moiety is assigned on the basis of $C_{\infty v}$ symmetry. [f] Lines attributed to the F–Xe--F bend and F_4–M--F bend are presumed to be coincident.

---

(8) Tucker, P. A.; Taylor, P. A.; Holloway, J. H.; Russell, D. R. *Acta Crystallogr., Sect. B* **1975**, *31*, 906.

Table III. Raman Frequencies (cm^{-1}) and Assignments for $XeF_2 \cdot 2MOF_4$ (M = Mo, W)

$XeF_2 \cdot 2MoOF_4$[a]	$XeF_2 \cdot 2WOF_4$[b]	approx descriptn
1039 (43), 1030 (20)	1052 (50), 1044 (24)	$\nu(M{=}O)$
750 (1), 734 (6), 726 (4), 715 (37), 711 sh, 700 (20), 684 (8), 669 (8), 656 (9), 593 (7)	720 (26), 684 (1), 672 (3), 662 (1), 624 (3)	$\nu(MF_4)$
575 (100)	585 (100)	$\nu(Xe{-}F)$
546 (1), 528 (2), 504 (0.5)	541 (1)	$\nu(MF_4)$
422 (9)	409 (5)	$\nu(Xe{--}F)$
388 (1), 382 (2), 324 sh, 314 (20)	332 (4), 324 (12), 317 (28), 310 (15)	$\nu(M{--}F)$, $\delta(F_4M{=}O)$
298 (10), 276 (1), 259 (2), 236 (6), 230 sh, 212 (4), 198 (2), 193 (1), 170 (1)	299 (6), 270 (0.5), 251 (0.5), 236 (3), 226 (3), 208 (3), 196 sh	$\delta(MF_4)$
156 (10)	154 (9)	$\delta(F{-}Xe{--}F)$
142 (4)	144 (5)	$\delta(F_4M{--}F)$
111 (3), 99 (2), 68 (12)	66 (15)	$\delta(M{--}F{--}M)$, torsional and lattice modes

[a] Recorded at -109 °C in an FEP sample tube. [b] Recorded at -100 °C in a glass sample tube.

been derived by assuming approximate $C_{\infty v}$ and C_{4v} symmetries for the NgF_2 and MOF_4 moieties, respectively. This assumption appears to be valid in view of the weak nature of the F---M bond in these adducts.

Assignments for the NgF_2 group have been derived by correlating the axially distorted NgF_2 molecule under $C_{\infty v}$ symmetry to the $D_{\infty h}$ symmetry of the free fluoride. These correlations have been elaborated on in a previous paper[3] and are presented along with their appropriate assignments in Table II. Four modes are expected for the distorted linear F–Ng---F group, the Ng–F stretching mode, the Ng---F stretching mode and the doubly degenerate F–Ng---F bending mode, all of which are active in the Raman. In related studies, ν(Ng–F), ν(Ng---F), and δ(F–Ng---F) have been assigned in the $NgF^+MF_6^-$ (M = As, Sb, Pt) compounds.[9] A comparison of the corresponding frequencies among MOF_4 (M = Mo, W) and MF_6^- (M = As, Sb, Pt) compounds[9] shows that the terminal Ng–F stretching frequency occurs at uniformly lower frequencies in the MOF_4 compounds while the stretching frequency of the longer Ng---F bond is at higher frequency than its fluoride-bridged counterpart in the MF_6^- and $M_2F_{11}^-$ species. We may, therefore, conclude that valence bond structures IVb and IVc are dominant for MOF_4 compounds while a greater degree of ionic character is evident in the MF_6^- and $M_2F_{11}^-$ compounds (structure IVa). This fluorine-bridged nature of the adducts is confirmed by the X-ray crystal structure determination of $XeF_2 \cdot WOF_4$,[8] in which the Xe---F bond (2.04 Å) is only marginally longer than the terminal Xe–F bond (1.89 Å) and the Xe–F bonds of free XeF_2 (2.00 Å).[10]

As an initial assumption, the MOF_4 groups in the 1:1 adducts can be regarded as having C_{4v} symmetry. Raman assignments have consequently been made on this basis and correlated to the molecular point symmetry C_s (Table II). We have chosen the compounds $Cs^+MOF_5^-$ [11] and $NO^+MOF_5^-$ [12] (M = Mo, W) as model systems upon which to base our assignments of F---MOF_4 group frequencies.

The M=O stretching frequency of $NgF_2 \cdot MOF_4$ is readily assigned to a band occurring in the 1020–1045-cm^{-1} region and is split due to factor-group effects. This band is consistently 50–65 cm^{-1} higher than in the corresponding MOF_5^- anion which is consistent with the greater M–O bond order anticipated in the neutral adduct. Similar observations apply to bridging M---F stretching frequencies of the complexes which occur 25–60 cm^{-1} lower than the corresponding mode in their respective anions. The remaining frequencies of the F---MOF_4 group have been assigned by analogy with their anion counterparts. Finally, we note that substantial factor-group splittings of the totally symmetric Ng—F, MF_4 and M=O stretching frequencies are observed for all cases studied.

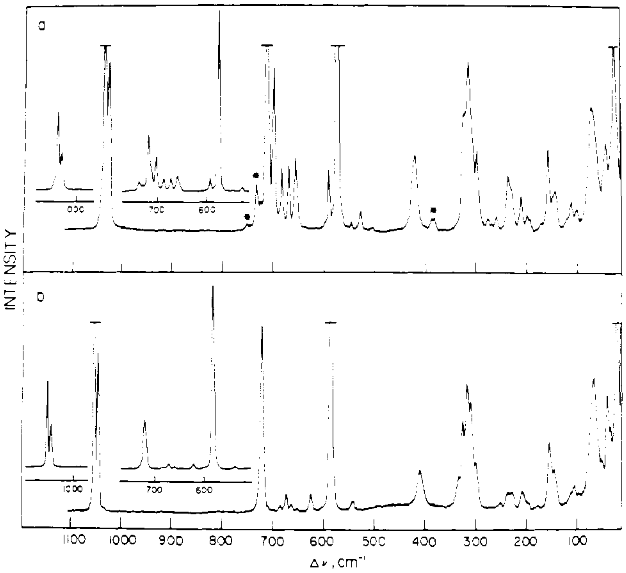

Figure 5. Raman spectra of (a) $XeF_2 \cdot 2MoOF_4$ (-114 °C) and (b) $XeF_2 \cdot 2WOF_4$ (-90 °C) (asterisks denote FEP sample tube lines).

$XeF_2 \cdot 2MoOF_4$ and $XeF_2 \cdot 2WOF_4$. Although the Raman spectra of $XeF_2 \cdot 2MOF_4$ cannot yet be fully assigned, some firm assignments and conclusions concerning the nature of these adducts can be made (Table III and Figure 5). We note that the only reported vibrational studies of an $M_2O_2F_9^-$ anion are those of Bougon and co-workers[12] and Beuter and Sawodny,[13] who have partially assigned the vibrational spectra of $Rb^+Mo_2O_2F_9^-$, $ClOF_2^+Mo_2O_2F_9^-$ and $NO^+M_2O_2F_9^-$ (M = Mo, W). The results of their work have been used to aid our assignments in Table III. Assignments for the XeF_2 group have again been derived by correlating the axially distorted XeF_2 molecule under $C_{\infty v}$ symmetry to $D_{\infty h}$ symmetry of the free molecule.

Two intense M=O stretches are observed in the 2:1 adducts, thus eliminating the possibility that the adducts isomerize giving Xe—O-bonded or M—O—M-bridged species in the solid state. It is not possible to distinguish between M=O

---

(9) Reference 3 and references therein.
(10) Levy, H. A.; Agron, P. A. *J. Am. Chem. Soc.* **1963**, *85*, 241.
(11) Beuter, A.; Sawodny, W. *Z. Anorg. Allg. Chem.* **1976**, *427*, 37.
(12) Bougon, R.; Bui Huy, T.; Charpin, P. *Inorg. Chem.* **1975**, *14*, 1822.
(13) Beuter, A.; Sawodny, W. *Angew. Chem., Int. Ed. Engl.* **1972**, *11*, 1020.

bonds which are trans–trans, cis–cis, or cis–trans to the fluorine of the M---F_d---M bridge by using Raman spectroscopy alone. Our ^{19}F NMR results for $XeF_2\cdot 2MOF_4$ and $KrF_2\cdot 2MoOF_4$ (discussed above), however, suggest that the oxygens are both trans and that the NgF group is cis to F_d in solution (structure II).

Only one band is observed in the 400–500-cm^{-1} region where ν(Ng---F) and ν(M---F) have both been observed in the 1:1 adducts. The single band in this region is assigned to ν(Xe---F) and is, by virtue of the increased ionic character of the Xe---F bond, lower in frequency than in its 1:1 analogues. The F---M---F stretching frequencies are expected to occur at significantly lower frequencies than in the 1:1 compounds and are consequently assigned to bands in the 300–400-cm^{-1} regions.

Enhancement of ionic character is evidenced in going from $XeF_2\cdot MOF_4$ to $XeF_2\cdot 2MOF_4$ and from M = Mo to M = W as is seen from an increase in their terminal Xe–F stretching frequency and a corresponding decrease in the bridging Xe---F stretching frequency (Tables II and III). These observations are consistent with our previous solution ^{129}Xe and ^{19}F NMR findings[2] for $XeF_2\cdot nMOF_4$ systems and parallel our NMR findings for the KrF_2 analogues (discussed above) in which we have noted an increase in NgF^+ character with increasing polynuclear MOF_4 chain length.

Experimental Section

Apparatus and Materials. All manipulations were carried out under anhydrous conditions on a vacuum line constructed from 316 stainless steel, nickel, Teflon, and FEP. All preparative work involving xenon and krypton compounds was carried out in 7-mm and 3.5-mm o.d. lengths of FEP spaghetti tubing, respectively. The tubing was heat sealed at one end and connected through a 45° SAE flare to a Kel-F valve to form the reaction vessel. Transfers of XeF_2, WOF_4, $MoOF_4$ and their solid adducts were carried out in a dry-nitrogen atmosphere in a drybox.

KrF_2,[14] XeF_2,[15] WOF_4,[2] and $MoOF_4$[2] were prepared as described elsewhere. Commercial SO_2ClF (Research Inorganic Chemicals) was subjected to further purification by vacuum distillation onto SbF_5 (Ozark-Mahoning) to remove traces of SO_2, an effective reducing agent toward XeF_2, KrF_2 and their compounds, followed by distillation onto NaF (dried at 300 °C under vacuum for 3 days) to remove traces of SbF_5 and HF. After standing over NaF for several days, the solvent was vacuum distilled into a dry glass storage vessel fitted with a Teflon Rotaflo valve.

The adducts $XeF_2\cdot MOF_4$ and $XeF_2\cdot 2MOF_4$ (M = Mo, W) were prepared by fusing stoichiometric amounts of XeF_2 and MOF_4 together at 50–60 °C to give clear, colorless liquids which crystallized at room temperature. In typical preparations, the following amounts of reactants were used: $XeF_2\cdot WOF_4$, 4.28 mmol of XeF_2 and 4.25 mmol of WOF_4; $XeF_2\cdot 2WOF_4$, 3.90 mmol of XeF_2 and 7.77 mmol of WOF_4; $XeF_2\cdot MoOF_4$, 6.46 mmol of XeF_2 and 6.32 mmol of $MoOF_4$; $XeF_2\cdot 2MoOF_4$, 5.68 mmol of XeF_2 and 11.35 mmol of $MoOF_4$.

The KrF_2/MOF_4 adducts were prepared in SO_2ClF solution by condensing ca. 0.3 g of SO_2ClF onto ca. 0.10 g of oxide tetrafluoride in 3.5-mm o.d. reaction vessels. For the preparation of the 1:1 adducts, approximately a 25% excess of KrF_2 was condensed into the reaction vessel at −196 °C and the tube and contents were warmed to −80 °C to effect reaction. The WOF_4 system was found to react vigorously at this temperature evolving Kr, O_2, and WF_6 and had to be periodically quenched with liquid nitrogen and pumped to remove Kr and O_2 gases. This reaction was found to be particularly vigorous when a stoichiometric excess of WOF_4 was employed. In the latter instance, the reaction went to completion in a few seconds at −80 °C, yielding only WF_6 and WOF_4 in solution. In contrast, $MoOF_4/KrF_2$ solutions of any stoichiometry could be briefly warmed to room temperature to effect complete dissolution with no apparent further reaction. These solutions were cooled to −48 °C, and the solvent was removed under vacuum. Solvent and WF_6 formed in the WOF_4/KrF_2 system were likewise removed at −48 °C. Both solid 1:1 adducts were consequently isolated with small excesses of KrF_2 which were subsequently removed by brief pumping at 0 °C.

The purities of all solid adduct preparations were assessed by low-temperature Raman spectroscopy.

Sample Preparation. Nuclear magnetic resonance samples where $MOF_4:KrF_2 > 1$ were prepared in 5-mm o.d. precision glass NMR tubes (Wilmad) joined to $^1/_4$-in. o.d. standard wall tubing and attached by means of $^1/_4$-in. Teflon nuts and ferrules to a Teflon diaphragm valve. Samples containing $MOF_4:KrF_2 = 1$ were prepared in their respective 3.5-mm o.d. FEP reaction vessels (described above) by condensing SO_2ClF at −196 °C onto the solid adduct after its low-temperature Raman spectrum had been recorded. All samples containing $MoOF_4$ were warmed briefly to room temperature while samples containing $KrF_2\cdot WOF_4$ and excess WOF_4 were warmed to −48 and −80 °C, respectively, for a few seconds to effect reaction and/or dissolution. Sulfuryl chlorofluoride was vacuum distilled through all Kel-F and Teflon connections into a sample tube containing the solute(s) at −196 °C. All samples were heat sealed under vacuum. Sealed FEP sample tubes were inserted into 5-mm o.d. thin-wall precision NMR tubes when spectra were run.

Raman spectra were obtained in either vacuum sealed glass or FEP sample tubes. All samples were stored at −196 °C until their spectra could be recorded.

^{19}F NMR Spectroscopy. Fluorine-19 NMR spectra were obtained with the use of a Bruker WH-90 Fourier-transform multinuclear spectrometer equipped with a Nicolet 1080 computer, a Nicolet 294 desk memory, and quadrature phased detection. All ^{19}F spectra were ^2H locked by using an external D_2O lock and accumulated in a 16-K memory. Spectra were recorded at 84.66 MHz in 300–400 scans with use of a spectral width of 30 kHz (3.7 Hz per data point; pulse repetition time 0.270 s) and a pulse width of 2 μs. Variable-temperature studies were carried out with the use of a Bruker temperature controller. Temperatures were measured with use of a copper–constantan thermocouple inserted directly into the sample region of the probe and were accurate to ±1 °C.

The chemical shift convention is that outlined by IUPAC,[16] i.e., a positive chemical shift denotes a positive frequency and vice versa with respect to the designated reference substance. All ^{19}F spectra were referenced with respect to neat $CFCl_3$ at the quoted sample temperature.

Laser Raman Spectroscopy. A Spectra Physics Model 164 argon ion laser giving up to 900 mW at 5145 Å was used to excite the Raman spectra. The spectrometer was a Spex Industries Model 14018 double monochromator equipped with 1800 grooves/mm Holographic gratings. An RCA C31034 phototube detector in conjunction with a pulse count system consisting of pulse amplifier, analyzer, and rate meter (Hamner NA-11, NC-11 and N-780A, respectively) and a Texas Instruments FSOZWBA strip chart recorder were used to record the spectra. The spectrometer was periodically calibrated by recording the discharge lines from an argon lamp over the spectral range of interest; the Raman shifts quoted are estimated to be accurate to ±1 cm^{-1}. Slit widths depended on the scattering efficiency of the sample, laser power, etc., with 100 μm being typical.

Cylindrical sample tubes were mounted vertically. The angle between the incident laser beam and the sample tube was 45°, and Raman scattered radiation was observed at 45° to the laser beam or 90° to the sample tube direction.

Low-temperature spectra were recorded by mounting the sample vertically in an unsilvered Pyrex glass Dewar filled with liquid nitrogen or by passing a stream of cold nitrogen gas through the Dewar.

Registry No. $KrF_2\cdot MoOF_4$, 77744-88-8; $KrF_2\cdot 2MoOF_4$, 77744-89-9; $KrF_2\cdot 3MoOF_4$, 77744-90-2; $KrF_2\cdot WOF_4$, 77744-91-3; $XeF_2\cdot MoOF_4$, 74080-83-4; $XeF_2\cdot WOF_4$, 55888-48-7; $XeF_2\cdot 2MoOF_4$, 65651-37-8; $XeF_2\cdot 2WOF_4$, 56174-65-3; $MoOF_4$, 14459-59-7; WOF_4, 13520-79-1; KrF_2, 13773-81-4; XeF_2, 13709-36-9.

---

(14) Schreiner, F.; Malm, J. G.; Hindman, J. C. *J. Am. Chem. Soc.* **1965**, *87*, 25.

(15) Williamson, S. M. *Inorg. Synth.* **1968**, *11*, 147.

(16) "Recommendations for the Presentation of NMR Data for Publication in Chemical Journals". *Pure Appl. Chem.* **1972**, *29*, 627; **1976**, *45*, 217.